



## Chlorophenol electrooxidation on iron oxide-covered aluminosilicates deposited on glassy carbon

M.S. URETA-ZAÑARTU<sup>1,\*</sup>, M.L. MORA<sup>2</sup>, M.C. DIEZ<sup>3</sup>, C. BERRÍOS<sup>1</sup>, J. OJEDA<sup>1</sup> and C. GUTIÉRREZ<sup>4</sup>

<sup>1</sup>Facultad de Química y Biología, Universidad de Santiago de Chile, Casilla 40, correo 33, Santiago, Chile

<sup>2</sup>Dpto. de Ingeniería Química, Universidad de la Frontera, Temuco, Chile

<sup>3</sup>Dpto. Ciencias Químicas, Universidad de la Frontera, Temuco, Chile

<sup>4</sup>Instituto de Química-Física “Rocasolano” CSIC, España

(\*author for correspondence, e-mail: mureta@lauca.usach.cl)

Received 5 March 2002; accepted in revised form 4 July 2002

**Key words:** chlorophenols electrooxidation, modified GC electrodes

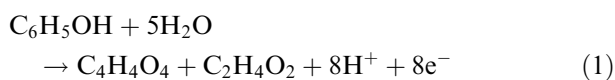
### Abstract

The electrooxidation, at different pH values, of several chlorophenols on porous electrodes obtained by painting commercial glassy carbon (GC) electrodes with a suspension of graphite powder and an iron oxide-covered aluminosilicate (AlSiFe) has been studied. Samples of the AlSiFe suspension were characterized by electrophoretic migration, and the dried powder was analysed by FTIR and XPS spectroscopy. The conductivity of the modified GC electrode was corroborated by cyclic voltammetry of the ferro-ferricyanide couple. The influence of the chlorophenol structure on the reactivity of the phenols was studied.

### 1. Introduction

There is considerable interest in the determination and degradation of phenolic compounds in the environment, in industrial products and in foods. Diverse materials have been tried in the quest for electrodes on which phenol mineralization is complete and electrode fouling due to phenol polymerization is absent. [1–5]. In previous work we have studied chlorophenol oxidation on gold electrodes in acid media [6] and on glassy carbon (GC) electrodes at different pH [7]. On gold, oxidation of all the chlorophenols (CPs) started together with the oxidation of gold, which indicates that gold oxocompounds are electrocatalysts for CP oxidation. EQCM measurements allowed estimation of the CP polymerization rate, which was a function of the CP structure. With the GC electrode the voltammetric peak potential depended on the CP structure: there was a negative linear correlation between the peak potential and the *pK<sub>a</sub>*. CPs with one or two chlorine atoms fouled the GC electrode, while tri- and penta-CPs did not.

Electrooxidation of chlorophenols is very complex [8]. Electrooxidation of phenol has been assumed to proceed according to the following reaction [9]



The  $\text{C}_2\text{H}_4\text{O}_2$  species is an unstable compound, leading to glyoxal and glyoxalic, oxalic and formic acids [9]. In general, electrooxidation of organic compounds requires OH or O groups on the metal surface, as occurs with Pt [10].

Tahar et al. [4] reported that galvanostatic electrooxidation of phenol at pH 2 on Ta/PbO<sub>2</sub> anodes yielded hydroquinone, catechol, 1,4-benzoquinone, maleic and fumaric acids and carbon dioxide as the main products. Pham et al. [11] detected the phenoxy radical during the anodic oxidation of 2,6-disec-butyl phenol on iron by multiple internal reflection Fourier transform infrared spectroscopy (MIRFTIRS). Iniesta et al. [12] and Hagens et al. [13] electrooxidized phenol in acid media using boron-doped diamond electrodes. Iniesta et al. [12], working with 2.5–20 mM phenol in 1 M HClO<sub>4</sub> reported electrode fouling in the potential region of water stability. However, in the oxygen evolution region ( $E > 2.3$  V vs SHE) they obtained an indirect oxidation of phenol, probably mediated by hydroxyl radicals, without electrode fouling, and with the possibility of controlling the reaction products (CO<sub>2</sub> and aromatics compounds) by a proper choice of the experimental conditions. Hagens et al. [13] working with an unspecified, but apparently similar, phenol concentration in 0.1 M H<sub>2</sub>SO<sub>4</sub> claimed that phenol was completely oxidized to CO<sub>2</sub> on the diamond electrodes without electrode fouling, even after prolonged cycling. Oturan [14, 15] obtained OH• radicals electrochemically using a carbon felt electrode on

which Fenton's reagent was produced by simultaneous reduction of dioxygen to hydrogen peroxide and of ferric to ferrous ions. These  $\text{OH}^\bullet$  radicals were used for elimination of organic pollutants in water through their transformation into biodegradable compounds or through their mineralization into  $\text{H}_2\text{O}$  and  $\text{CO}_2$ . Nadtochenko and Kiwi [16] have studied the reaction of Fe(III) from  $\text{FeCl}_3 \cdot 6\text{H}_2\text{O}$  or  $\text{Fe}(\text{ClO}_4)_3 \cdot 9\text{H}_2\text{O}$  with phenol in aqueous solution by nanosecond laser photolysis. They suggest that the mechanism leads to the formation of phenoxyl radical and involves the photooxidation of phenol by  $\text{Cl}^\bullet$  and  $\text{Cl}_2^{\bullet-}$ .

Allophanic soil has been successfully used in wastewater treatment for removing chlorinated phenol compounds [17]. The main clay component in Chilean Andisols is allophane [18] with a specific surface of 700 to  $800 \text{ m}^2 \text{ g}^{-1}$ . Specific interaction of CPs with the Al oxide, where the phenolic hydroxyl group could be directly involved in surface complexation, has been suggested [19].

In this work we have studied the activity for the oxidation of chlorophenols of glassy carbon electrodes modified with aluminosilicates (similar to synthetic allophane) onto which an iron oxide had been precipitated.

## 2. Experimental details

### 2.1. Preparation of aluminosilicates

Aluminosilicates (Al-Si) similar to natural allophane were synthesized by mixing 80 mL of 1.11 M aluminium chloride solution and 104 mL of a 1.3 M potassium silicate solution, at pH near 5.0 and 25 °C. Small changes in the pH of the solution yield aluminosilicates with different Al/Si ratios as evaluated by the isoelectric point (below). Samples with three Al/Si ratios were prepared to evaluate the role of this ratio on the catalytic activity of the modified electrodes. This yielded an aluminosilicate precipitate which was centrifuged, and onto which iron oxide was precipitated by immersion in an aqueous solution of  $\text{Fe}(\text{NO}_3)_3 \cdot 9\text{H}_2\text{O}$  (5 g for 300 mL final solution), that is, by impregnation with a solvent excess. The iron oxide-covered aluminosilicate (in the following designated as AlSiFe) was centrifuged and washed three times with 1 M KCl, and then with bidistilled water until no chloride anion was detected, and the suspension was stored in a plastic bottle.

### 2.2. Characterization of the aluminosilicate samples

The Al, Si and Fe contents of the aluminosilicate samples was determined by atomic absorption spectrophotometry [20]. The isoelectric point (IEP) is the pH value at which the zeta potential is zero [21, 22]. It was determined with a suspension containing 30 mg of dried powder near  $2 \mu\text{m}$  in diameter in 300 mL of 1 mM KCl solution. The pH was adjusted with 0.2 M KOH and/or 0.2 M HCl solutions. A Zeta-Meter Inc. (model 3.0+)

instrument provided with an autosampler was used [23].

Infrared spectra were obtained with an FTIR Bruker (IFS 66 V) spectrophotometer.

The XPS data were recorded at a take-off angle of 90° with a triple channeltron CLAM2 analyser using  $\text{AlK}_{\alpha}$  radiation and a constant transmission energy of 100 eV for the wide scan spectra, and 20 eV for the narrow spectra. The XP spectra were computer fitted.

### 2.3. Electrode preparation

The GC electrode ( $0.5 \text{ cm}^2$  geometric area) was modified with 0.5 mL of a mixture obtained by mixing and ultrasonically homogenizing 50 mg of graphite (fine powder, Riedel de Haën), 1.5 mL of Nafion® perfluorinated ion-exchange resin (Aldrich) and 4 mL of an aqueous suspension of AlSiFe (Table 1 for the Fe content). As a blank, a similar solution with graphite powder, 1.5 mL of Nafion® perfluorinated ion-exchange resin and 4 mL of water was used. The solvent was evaporated in air at a controlled temperature (25–80 °C) for a few hours, as in the work of Gloaguen et al. [24]. The graphite powder was previously cleaned by heating in an argon atmosphere at 120 °C for 4 h, and cooled and stored under nitrogen in a desiccator.

### 2.4. Electrochemical measurements

The electrochemical measurements were carried out in a conventional three-compartment electrochemical cell at room temperature and under nitrogen. The chlorophenols studied were 2- and 4-chlorophenol (2-CP and 4-CP), 2,4- and 2,6-dichlorophenol (2,4-DCP and 2,6-DCP), 2,4,6-trichlorophenol (2,4,6-TCP) and pentachlorophenol (PCP), all Aldrich p.a., which were used as received.

A  $\text{Hg}/\text{Hg}_2\text{SO}_4/\text{Na}_2\text{SO}_4$  (saturated) electrode (MSE) was used as reference and a platinum wire as auxiliary electrode. All potentials are referred to the MSE (0.68 V vs SHE). The electrode potential was controlled by a Wenking (POS 73) potentiostat interfaced to a CAEM data acquisition system with real-time data acquisition software.

### 2.5. Analysis of reaction products

For gas chromatography mass spectroscopy (GCMS) analysis the samples were saturated with NaCl, and then

Table 1. IEP values of aluminosilicate (AlSi) and iron oxide-covered aluminosilicate (AlSiFe) samples in 1 mM KCl in the presence and absence of 1 mM 2,4,6-TCP

	Sample I	Sample II	Sample III
Al-Si	2.2	9.2	4.4
Al-Si-(2,4-DCP)	–	–	3.8
Al-Si-Fe	3.2 (5% Fe)	8.2 (5% Fe)	5.1 (6.2% Fe)
Al-Si-Fe-(2,4-DCP)	3.0 (5% Fe)	–	7.2 (6.2% Fe)

extracted with ethyl ether. The organic phase was dried at 50 °C under a nitrogen atmosphere and derived with methylsililtrifluoroacetamide (MSTFA). The derived mixture was injected at the GCMS, a signal at 12.4 min being obtained for the derived 2,4,6-TCP.

### 3. Results and discussion

#### 3.1. Characterization of the synthetic allophanes

##### 3.1.1. FTIR spectroscopy

FTIR spectra of KBr pellets of aluminosilicate and AlSiFe samples are given in Figure 1. The aluminosilicate sample shows the characteristic bands at 1130–1000  $\text{cm}^{-1}$  due to asymmetric Si–O–Si stretching, and at 3700–3200  $\text{cm}^{-1}$  due to the Si–OH and Al–OH groups [25]. The presence of iron oxide did not substantially change the spectra. In spectra of aluminosilicate and AlSiFe samples pelletized together with graphite, the peaks did not change although obviously the transmittance decreased. Graphite powder showed no bands.

##### 3.1.2. Electrophoretic migration

The IEPs of the aluminosilicate and of AlSiFe (iron oxide-coated aluminosilicate) in the presence and absence of 2,4,6-TCP are given in Table 1. The iron oxide coating did not significantly affect the IEP of the acidic aluminosilicate sample I, increased slightly the IEP of the slightly acidic sample III, and decreased the IEP of the slightly basic sample II. The slightly acidic AlSiFe of sample III showed a good interaction with phenol, since this increased its IEP by two pH units. The  $\text{SiO}_2/\text{Al}_2\text{O}_3$  molar ratio for sample III was 2.2. This sample was mainly used in this study because it yielded AlSiFe-GC electrodes with good catalytic activity and its  $\text{SiO}_2/\text{Al}_2\text{O}_3$  molar ratio is very similar to that of the allophanic soil constituting Chilean Andisol.

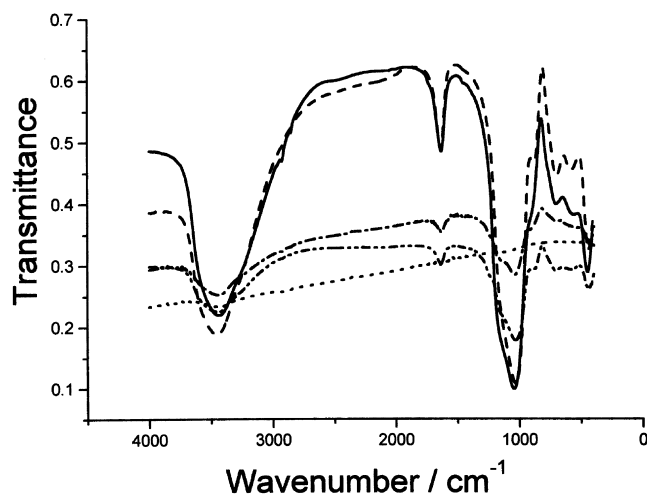


Fig. 1. Transmission FTIR spectra. Key: (—) AlSi-Fe, (---) AlSi, (- - -) graphite, (- - -) graphite-AlSi-Fe, (- - -) graphite-AlSi.

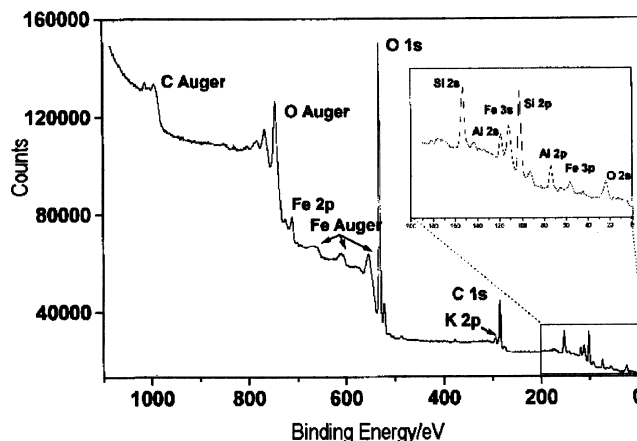


Fig. 2. XP spectrum of a pelletized sample of an aluminosilicate coated with iron oxide. Inset corresponds to enlarged signal between 0 and 200 eV.

##### 3.1.3. XPS spectra

The XPS spectrum of the AlSiFe sample III (Figure 2) shows the presence of O, Al, Si, Fe and some K. Iron was present as  $\text{Fe}^{2+}$  (67%) and  $\text{Fe}^{3+}$  (33%).

#### 3.2. Evaluation of the conductivity of the iron oxide-coated aluminosilicate deposited on glassy carbon (AlSiFe-GC) electrodes

Figure 3 shows CVs at 0.15  $\text{V s}^{-1}$  in 0.5 M KCl of GC (dashed line) and of an aluminosilicate-GC modified electrode (dotted line). The aluminosilicate produces an increase in the double layer charge, indicating a higher

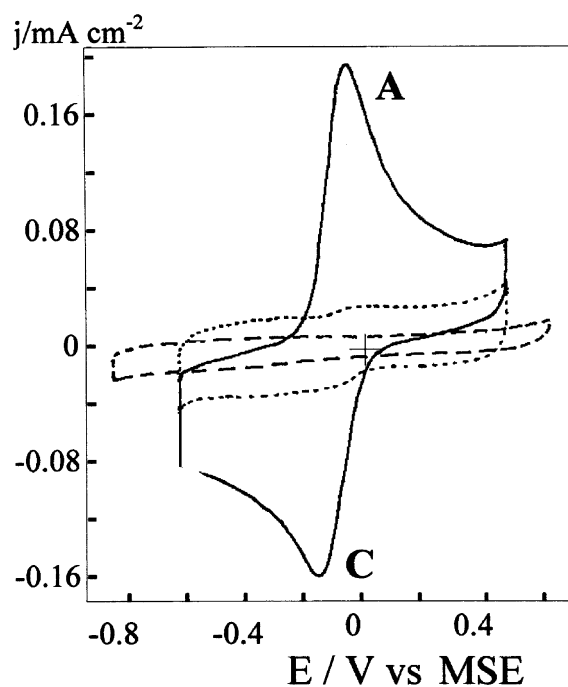


Fig. 3. Cyclic voltammograms at 0.15  $\text{V s}^{-1}$  of an aluminosilicate-GC electrode in 1 M KCl in the presence (solid line) and the absence (dotted line) of 1 mM  $\text{K}_4\text{Fe}(\text{CN})_6$ . Dashed line, bare GC electrode in 0.5 M KCl.

active electrode/solution interface area. The solid line is the CV, also at  $0.15 \text{ V s}^{-1}$ , of the aluminosilicate-GC modified electrode in  $0.5 \text{ M KCl} + 1 \text{ mM K}_4\text{Fe}(\text{CN})_6$ . The separation between the anodic and cathodic peaks of ferro/ferricyanide is similar to that obtained with a bare GC electrode, which indicates that the coating has a good conductivity. The  $I_p$  vs  $v^{0.5}$  plot (not shown) for the peak of ferrocyanide is linear for both aluminosilicate-GC and bare GC electrodes, indicating diffusion control [26].

More reproducible electrodes were obtained by drying the electrodes at  $40^\circ \text{C}$  for a longer duration (2 h).

The CVs of three AlSiFe-GC electrodes obtained under the same experimental conditions are very similar (Figure 4), indicating good reproducibility of the electrode preparation procedure. The half sum of the anodic and cathodic peak potentials is about  $-0.1 \text{ V}$  vs MSE, in fair agreement with the reversible standard potential of the Fe(II)/Fe(III) couple,  $E^\circ = 0.77 \text{ V}$  vs SHE ( $0.09 \text{ V}$  vs MSE). These peaks appear at the same potential as those of the Fe(II)/Fe(III) couple, which precludes the evaluation of the conductivity of AlSiFe-GC electrodes from a CV of the ferro-/ferricyanide couple. However, it is very unlikely that the iron oxide coating increases the resistance of the aluminosilicate.

With repetitive cycling the peaks become smaller, the peak current decreasing by 18% after five CVs.

The anodic peak potential increased by  $0.18 \text{ V}$  when the pH was increased from 2.2 to 7.0, while the cathodic peak potential remained constant.

### 3.3. Activity of iron oxide-coated aluminosilicate deposited on glassy carbon (AlSiFe-GC) electrodes for the electrooxidation of chlorophenols

Previous work in our laboratory [7] has shown that CPs are oxidized at the glassy carbon electrode, their

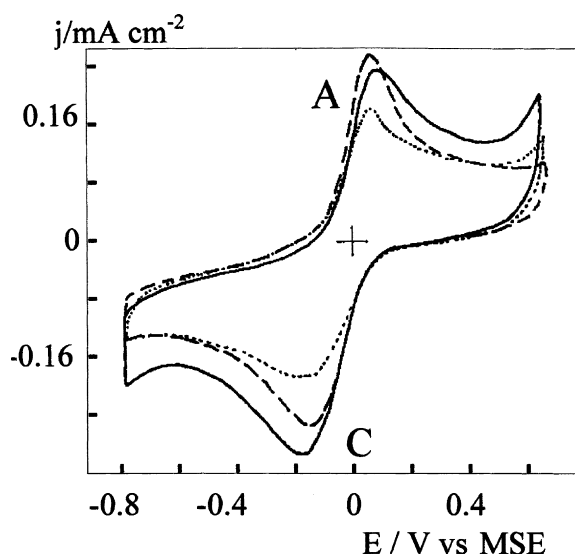


Fig. 4. Cyclic voltammograms at  $0.1 \text{ V s}^{-1}$  of three different iron oxide-coated aluminosilicate deposited on glassy carbon (AlSiFe-GC) electrodes at pH 2.2.

oxidation potential being dependent on the number and position of the chlorine atoms. Thus, molecules with less Cl substitution (those with a higher  $pK_a$ ) show a higher oxidation potential, and this potential is even higher if the substitution is in the *para* as compared with the *ortho* position.

First cyclic voltammograms at  $0.01 \text{ V s}^{-1}$  of a sample I AlSi-GC (A) and AlSiFe-GC (B) electrodes at pH 8.3 in the presence (solid line) and the absence (dotted line) of  $1 \text{ mM}$  2-CP are shown in Figure 5. Both electrodes show an anodic peak near  $0.15 \text{ V}$  that can be attributed to the well-known one-electron process of phenoxi radical formation [7]. The peak current is three times higher for the AlSiFe as compared with the AlSi electrode, indicating that the iron oxide is a catalyst for phenol electrooxidation.

3.3.1. Effect of the basicity of the aluminosilicate on the activity of iron oxide-coated aluminosilicate deposited on glassy carbon (AlSiFe-GC) electrodes  
Electrodes with the three AlSiFe samples (Table 1) were prepared and their activity at pH 2.2 for all the CPs studied was measured by cyclic voltammetry at  $0.1 \text{ V s}^{-1}$ . As an example, Figure 6 shows the first (solid line) and 5th (dashed line) CVs of the AlSiFe-GC electrodes in the presence and the absence (dotted line) of  $1 \text{ mM}$  4-CP (A, B and C) and 2,6-DCP (D, E and F).

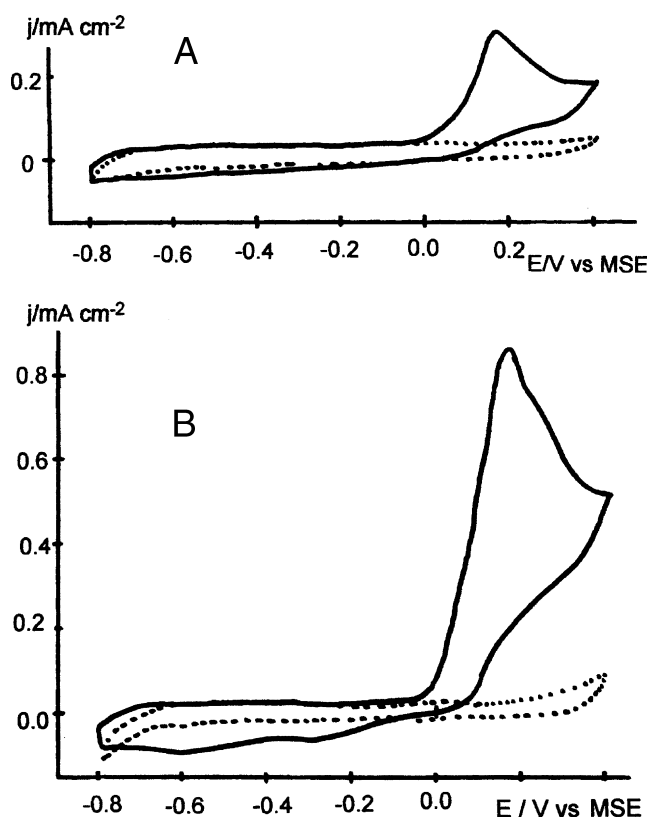


Fig. 5. First cyclic voltammograms at  $0.01 \text{ V s}^{-1}$  of a sample I aluminosilicate deposited on glassy carbon (AlSi-GC) electrode (A) and of an iron oxide-coated sample I aluminosilicate deposited on glassy carbon (AlSiFe-GC) electrode (B) at pH 8.3 in the presence (solid line) and the absence (dotted line) of  $1 \text{ mM}$  2-CP.

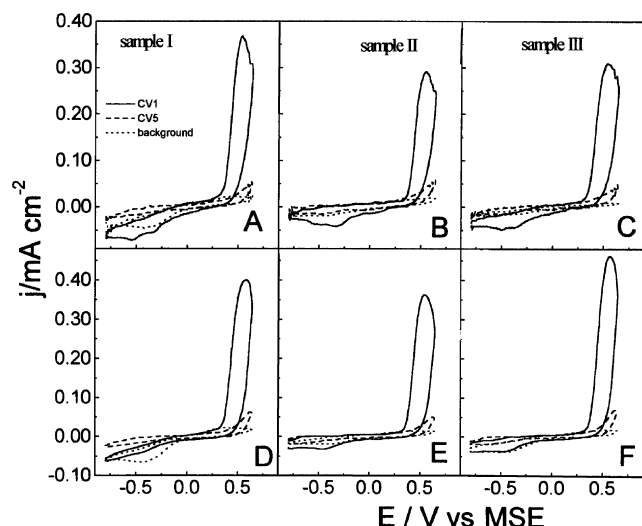


Fig. 6. First (solid line) and fifth (dashed line) voltammograms at  $0.1 \text{ V s}^{-1}$  of iron oxide-coated aluminosilicate deposited on glassy carbon (AlSiFe-GC) electrodes at pH 2.2 in the presence and the absence (dotted line) of 1 mM 4-CP (A, B and C) and 2,6-DCP (D, E and F) for three samples of AlSiFe prepared with the three aluminosilicates shown in Table 1.

No effect of the basicity of the different aluminosilicate samples could be observed. A similar voltammetric behaviour was observed for the other CPs, all CPs exhibiting a single irreversible peak on the three AlSiFe-GC electrodes.

The values of the peak potential and the peak current density of the anodic peak in CVs at  $0.1 \text{ V s}^{-1}$  of the six CPs on the three AlSiFe-GC electrodes are given in Table 2. 2-CP, 2,4- and 2,6-DCP and 2,4,6-TCP show a new anodic peak and a significant reduction current in the second scan (below). The anodic peak current

density is very dependent on the CP structure, decreasing in the order 4-CP > 2,4-DCP  $\approx$  2,6-DCP > 2,4,6-TCP > 2-CP > PCP. With mono- and di-CP fouling the electrode surface decreased dramatically the current density in repetitive scans, as can be seen in Figure 6, in which the 5th CV has been included. On the contrary, with 2,4,6-TCP and PCP the anodic peak current increased in the 2nd CV, and the electrode was not deactivated after five CVs.

### 3.3.2. Electrooxidation of 2,4-dichlorophenol

The activity of the AlSiFe-GC electrode for the oxidation of 2,4-dichlorophenol (2,4-DCP) was evaluated at pH values in the range 2–12. Figure 7 shows the 1st (solid line), 2nd (dashed line) and 15th (dashed-dotted line) CVs obtained with an AlSiFe-GC electrode (sample III) at  $0.1 \text{ V s}^{-1}$  in 1 mM 2,4-DCP at pH 2.2. The background CV is given as the dotted line. In the first positive scan a peak at 0.47 V (peak B) appears, together with a shoulder at the potential of the Fe(II)/Fe(III) peak, and in the negative scan the Fe(III)/Fe(II) reduction peak (peak C) increases and shows a prepeak. In the second CV (obtained immediately, without intermediate nitrogen bubbling) two new oxidation peaks appear at  $-0.05$  and  $+0.08 \text{ V}$  (peaks A), while peak B decreases. In subsequent CVs another anodic peak appears at 0.26 V (peak D). As for the cathodic peak near  $-0.1 \text{ V}$  (peak C), it increases with cycling and is shifted to more negative potentials. The 15th CV is already stabilized.

If, after 15 CVs, the AlSiFe-GC electrode was withdrawn from the 2,4-DCP solution, rinsed thoroughly with bidistilled water, and immersed in base electrolyte, the peaks of the Fe(III)/Fe(II) process decreased

Table 2. Peak potential ( $E_p$ ) and peak current density ( $j_p$ ) obtained by cyclic voltammetry at  $0.1 \text{ V s}^{-1}$  in the presence of 1 mM CP at pH 2.2 of AlSiFe-GC electrodes prepared with the three aluminosilicate samples shown in Table 1

CP	CV No.	Sample I		Sample II		Sample III	
		$E_p/\text{V}$	$I/\text{mA cm}^{-2}$	$E_p/\text{V}$	$I/\text{mA cm}^{-2}$	$E_p/\text{V}$	$I/\text{mA cm}^{-2}$
2-CP	1	0.612	0.213	0.607	0.230	0.607	0.221
	5*	0.627	0.111	0.634	0.104	0.629	0.099
4-CP	1	0.585	0.520	0.541	0.472	0.568	0.601
	5*	0.624	0.081	0.646	0.065	0.620	0.090
2,4-DCP	1	0.578	0.395	0.559	0.441	0.578	0.430
	5*	0.639	0.051	0.644	0.051	0.634	0.055
	5†	0.260	0.196	0.212	0.216	0.278	0.215
2,6-DCP	1	0.541	0.477	0.550	0.374	0.534	0.403
	5*	0.638	0.069	0.642	0.077	0.634	0.064
2,4,6-TCP	1	0.468	0.200	0.468	0.281	0.468	0.267
	5	0.539	0.213	0.512	0.272	0.522	0.259
	5†	0.174	0.023	0.189	0.452	0.174	0.038
PCP‡	1	0.520	0.030	0.537	0.278	0.529	0.042
	5	0.493	0.047	0.505	0.047	0.493	0.055

\* No peak in the 5th CV; potential shown corresponds to positive potential limit.

† Corresponds to the anodic peak that appears since the 2nd CV.

‡ Saturated solution.

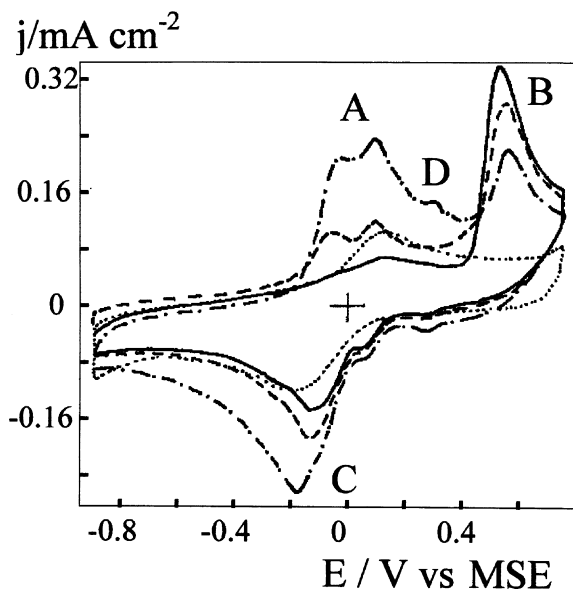


Fig. 7. First (solid line), 2nd (dashed line) and 15th (dashed-dotted line) cyclic voltammograms at  $0.1 \text{ V s}^{-1}$  of an iron oxide-coated aluminosilicate deposited on glassy carbon (AlSiFe-GC) electrode at pH 2.2 in the presence and the absence (dotted line) of 1 mM 2,4-DCP.

significantly. However, if the AlSiFe-GC electrode was left in air for 2 h, the CVs in base and in 2,4-DCP solutions almost fully recovered.

With nitrogen stirring of the electrolyte the CV tends to revert to the first CV, indicating that the species oxidized in the peaks II are soluble, and little, if any, phenol polymerization occurs. This behaviour is opposite to that obtained with a GC electrode, where 2,4-DCP oxidation passivated the electrode after only five scans [7].

In Figure 8 plots of the peak potentials (A) and the peak currents (B) for the anodic and cathodic processes in CVs at  $0.1 \text{ V s}^{-1}$  in the presence of 1 mM 2,4-DCP at different pH values are given. The dispersion of the results was not unexpected, since each point corresponds to a fresh electrode. For both peaks  $E_p$  shifts linearly to less positive potentials with increasing pH, with a slope near  $-50 \text{ mV dec}^{-1}$ , although for the anodic process  $E_p$  remains constant at pHs higher than 9. At the bare GC electrode the anodic slope is  $-60 \text{ mV dec}^{-1}$  [7].

### 3.3.3. Electrooxidation of 2,4,6-TCP

The CVs at  $0.1 \text{ V s}^{-1}$  in base electrolyte (dotted line) and in the presence of 1 mM 2,4,6-TCP at three pH values, 2.2, 5.3 and 10.6, are given in Figure 9. The CV shows an anodic peak that shifts to less positive potentials with increasing pH, and a cathodic peak whose potential is little affected by pH. The second scan (dashed line) shows an increase in the anodic peak current, but this is followed by a decrease in the subsequent scan. At pH 2.2 the anodic peak current after five CVs is the same as in the first CV (Table 2). In repetitive CVs there is a current increase near 0.0 V, similar to that observed with 2,4-DCP.

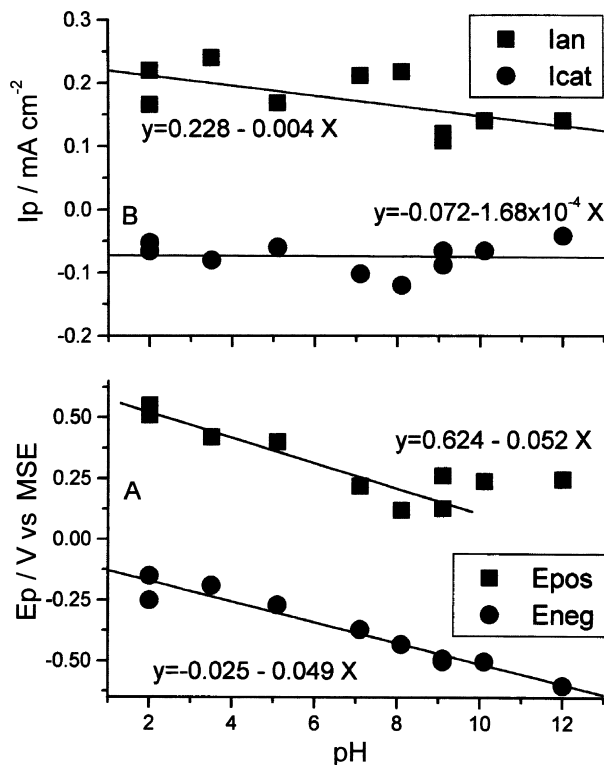


Fig. 8. Peak potentials ( $E_p$ ) and peak currents ( $I_p$ ) of the anodic peak (peak B in Figure 7) and cathodic peak (peak C) for the 1st cyclic voltammogram at  $0.1 \text{ V s}^{-1}$  of an iron oxide-coated aluminosilicate deposited on glassy carbon (AlSiFe-GC) electrode in 1 mM 2,4-DCP as a function of pH over the range pH 2–12.

Repetitive CVs at  $0.1 \text{ V s}^{-1}$  with an AlSiFe-GC electrode (sample III) in 1 mM 2,4,6-TCP at pH 2.2 were run for 10 h to analyse the soluble reaction products, changing the working electrode when it became deactivated. Although the final 2,4,6-TCP concentration, determined by GCMS, decreased by 75%,

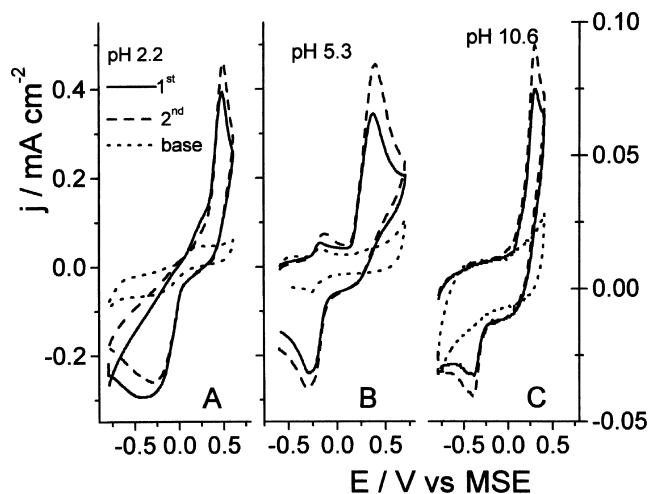


Fig. 9. First (solid line) and 2nd (dashed line) cyclic voltammograms at  $0.1 \text{ V s}^{-1}$  of an iron oxide-coated aluminosilicate deposited on glassy carbon (AlSiFe-GC) electrode in the presence and in the absence (dotted line) of 1 mM 2,4,6-TCP at (A) pH 2.2; (B) pH 5.3 and (C) pH 10.6.

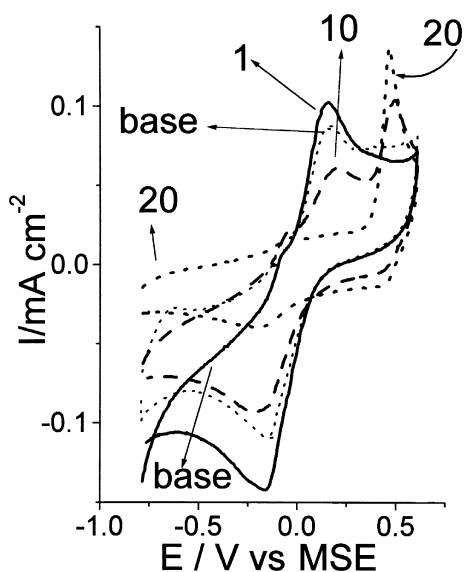


Fig. 10. Cyclic voltammograms at  $0.1 \text{ V s}^{-1}$  of an iron oxide-coated aluminosilicate deposited on glassy carbon (AlSiFe-GC) electrode in saturated PCP solution at pH 2.2. Voltammogram number: (—) 1, (---) 10, (· · · ·) 20 and (- · - ·) base.

no soluble reaction products were detected. Addition of aqueous  $\text{AgNO}_3$  to the electrolysis solution failed to yield the white precipitate characteristic of the chloride anion. It was found that the initial 2,4,6-TCP was contaminated with tetrachlorophenol, and that this contaminant decreased during the electrolysis. These results indicate that under the experimental conditions used the reaction products have a molecular weight high enough to preclude their volatilization, or that complete mineralization of the CPs was achieved.

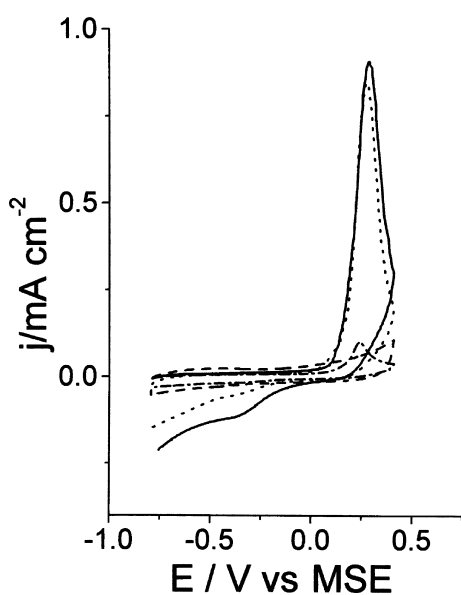


Fig. 11. Cyclic voltammograms at  $0.1 \text{ V s}^{-1}$  of an iron oxide-coated aluminosilicate deposited on glassy carbon (AlSiFe-GC) electrode in saturated PCP solution at pH 10. Voltammogram number: (—) 1, (---) 2, (· · · ·) 7 and (- · - ·) base.

### 3.3.4. Electrooxidation of pentachlorophenol

Pentachlorophenol (PCP) shows interesting behaviour at pH 2.2, as can be seen in Figure 10, where CVs at  $0.1 \text{ V s}^{-1}$  in base electrolyte (dashed line) and for PCP-saturated solution are shown. The first CV (solid line) shows a slight increase of the Fe(II)/Fe(III) anodic peak at 0.15 V, indicating some electro-oxidation of PCP, and also an increase of the reduction peak of Fe(III) in the negative scan. In the second CV both peaks increase, but in repetitive CVs the current decreases and a new anodic peak appears at 0.47 V, a potential very similar to that observed for PCP at bare GC [7]. The 20th CV is stabilized, with the Fe(III)/Fe(II) couple barely appearing, it being impossible to reactivate this process. No electrode fouling was observed.

At pH 10 only one anodic peak was observed near 0.3 V, and the Fe(II)/Fe(III) process became passivated after seven CVs (Figure 11).

## 4. Discussion

It should be stressed that the preparation procedure yielded AlSiFe-GC electrodes with a fairly reproducible electrochemical behaviour, which is a necessary condition for the development of useful electrodes. Aluminosilicates with several  $\text{SiO}_2/\text{Al}_2\text{O}_3$  ratio (evaluated by means of the IEP, which decreases monotonically with increasing  $\text{SiO}_2/\text{Al}_2\text{O}_3$  ratio) [18] yielded AlSiFe-GC electrodes with about the same catalytic activity for electrooxidation of the CPs, showing that the basicity of the aluminosilicate substrate did not affect the electrooxidation process. However, the aluminosilicate samples with an IEP of 4.4, which corresponds to an  $\text{SiO}_2/\text{Al}_2\text{O}_3$  molar ratio of 2.2, was preferentially used because this ratio is very similar to that of the allophanic soil constituting Chilean Andisol, which thus can be seen as an interesting proposal for the solution of environmental problems.

The results clearly show that CPs can be oxidized on AlSiFe-GC electrodes. The CVs of all tested CPs show an anodic peak between 0.45 and 0.61 V at pH 2.2, but the initial activity depends on the CP structure. So, while 2,4-DCP shows this peak already in the first sweep (Figure 7), at this acidic pH PCP shows it only after cycling (Figure 10), although at pH 10 PCP shows a large anodic peak at this potential already in the first CV (Figure 11). The structure of the CP also influences the extent of its electrooxidation and the passivation of the electrode, due to a polymerization that involves the phenoxi radical, as is well known.

The electrooxidation of CPs is probably mediated by Fe(III) surface species which are immediately reoxidized, the surface iron acting as a redox mediator between the CP and the electrode, as in the case of electrodes modified with organometallic complexes [27] such as metal phthalocyanines [28].

GCMS analysis failed to detect any reaction products after prolonged electrooxidation (10 h) of 2,4,6-TCP,

which suggests that a fraction of the reacted CP is completely mineralized, while the remainder is polymerized onto the electrode surface, which becomes passivated, this polymeric layer being undetectable by GCMS. No chloride ion was detected in the electrolyte, which indicates that dechlorination of the CP does not occur to a significant extent.

## 5. Conclusions

- (i) Preparation of AlSiFe-GC electrodes with a very reproducible behaviour was achieved.
- (ii) XP spectra of AlSiFe-GC electrode indicates that two thirds of the Fe atoms are present as Fe(II) ions.
- (iii) Electrooxidation of mono-, di-, tri- and penta-CPs at AlSiFe-GC electrodes has been achieved. Two main reaction pathways apparently occur: complete mineralization to CO<sub>2</sub>, and polymerization into a film that passivates the electrode surface.
- (iv) Tri- and penta-chlorophenols showed less electrode fouling, that is, a smaller rate of polymerization, than the other CPs after repetitive potential cycling.

## Acknowledgements

The authors thank Dicyt-USACH and FONDECYT (grant 1980378) for financial support. They also thank Dr J.R. Gancedo and Dr J.F. Marco (Instituto de Química-Física Rocasolano, CSIC, Madrid) for the XP spectra.

## References

1. M. Gattrell and D.W. Kirk, *J. Electrochem. Soc.* **140** (1993) 1534.
2. M. Gattrell and D.W. Kirk, *J. Electrochem. Soc.* **139** (1992) 2736.
3. P.I. Iotov and S.V. Kalcheva, *J. Electroanal. Chem.* **442** (1998) 19.
4. N.B. Tahar and A. Savall, *J. Electrochem. Soc.* **145** (1998) 3427.
5. A. Alvarez-Gallegos and D. Pletcher, *Electrochim. Acta* **44** (1999) 2483.
6. M.S. Ureta-Zañartu, P. Bustos, M.C. Diez, M.L. Mora and C. Gutiérrez, *Electrochim. Acta* **46** (2001) 2545.
7. M.S. Ureta-Zañartu, C. Berrios, P. Bustos, M.C. Diez, M.L. Mora and C. Gutiérrez, *Electrochim. Acta* **47** (2002) 2399.
8. M. Gattrell and B. MacDougall, *J. Electrochem. Soc.* **146** (1999) 3335.
9. N.B. Tahar and A. Savall, *J. Electrochem. Soc.* **145** (1998) 3427.
10. J.-L. Boudenne, O. Cerclier and P. Bianco, *J. Electrochem. Soc.* **145** (1998) 2763.
11. M.C. Pham, F. Adami and P.C. Lacaze, *J. Electrochem. Soc.* **136** (1989) 677.
12. J. Iniesta, P.A. Michaud, M. Panizza, G. Cerisola, A. Aldaz and Ch. Cominellis, *Electrochim. Acta* **46** (2001) 3573.
13. P.L. Hagan, P.M. Natishan, B.R. Stoner and W.E. ÖGrady, *J. Electrochem. Soc.* **148** (2001) E298.
14. M.A. Oturan, *J. Appl. Electrochem.* **30** (2000) 475.
15. M.A. Oturan, N. Oturan, C. Lahitte and S. Trevin, *J. Electroanal. Chem.* **507** (2001) 96.
16. V.A. Nadochenko and J. Kiwi, *J. Chem. Soc. Perkin Trans. 2* (1998) 1303.
17. M.C. Diez, M.L. Mora and S. Videla, *Water Res.* **33** (1999) 125.
18. M.L. Mora, M. Escudey and G. Galindo, *Bol. Soc. Chil. Quim.* **39** (1994) 237.
19. K.H. Kung and M.B. McBride, *Environ. Sci. Technol.* **25** (1991) 702.
20. B. Bernas, *Anal. Chem.* **40** (1964) 1682.
21. G.A. Parks, *Chem. Rev.* **65** (1965) 177.
22. R.J. Hunter, 'Zeta Potential in Colloid Science. Principles and Applications', (Academic Press, New York, 1981), p. 72.
23. F.J. Gil-Llambias and A.M. Escudey-Castro, *J. Chem. Soc. Chem. Commun.* (1982) 478.
24. F. Gloaguen, J.-M. Leger and C. Lamy, *J. Appl. Electrochem.* **27** (1997) 1052.
25. N.B. Colthup, L.H. Daly and S.E. Wiberley, 'Introduction to Infrared and Raman Spectroscopy' (Academic Press, San Diego, CA, 3rd edn, 1990), chapter 12.
26. A.J. Bard and L.R. Faulkner, 'Electrochemical Methods. Fundamentals and Applications' (John Wiley & Sons, New York, 1980), chapter 6.
27. I.G. Casella and M. Gatta, *Anal. Chem.* **72** (2000) 2969.
28. J.H. Zagal, *Coord. Chem. Rev.* **119** (1992) 89.